JOURNAL OF MATERIALS SCIENCE 27 (1992) 697–703

Active to passive transition in the oxidation of silicon carbide at high temperature and low pressure in molecular and atomic oxygen

M. BALAT, G. FLAMANT, G. MALE, G. PICHELIN
Institut de Science et de Génie des Matériaux et Procédés, IMP-CNRS, BP 5 Odeillo, 66120 Font-Romeu, France

The active to passive transition in the oxidation of sintered α-SiC has been determined by a thermodynamic approach and then experimentally under flowing air at high temperatures (1673–1973 K) and low pressures (oxygen partial pressure from 200–2100 Pa). Then, the physico-chemical behaviour of samples was compared for two different environments such as air-plasma atmosphere generated by microwaves, and a molecular atmosphere. The thermodynamic calculation does not predict any variation of the oxidation transition when changing the chemical state of oxygen (O_2 or O) but experimentally the domain characterized by the formation of a passive layer of silica is extended to lower pressure under atomic oxygen (for the same temperature range) than in the case of molecular oxygen.

1. Introduction

During the atmospheric reentry of hypersonic vehicles, the shock wave produces excited species such as ions, atoms, molecules and electrons which lead to very extensive damage to the thermal protective coating materials of the space shuttle (nose cap and wing leading edges).

In addition to this chemical attack, a large temperature increase in the protective shield is superimposed due to the thermal heat fluxes of between 0.5 and 1 $MW\,m^{-2}$. For the *Hermes* shuttle, this leads to maximal temperatures of 1773 K for the wing leading edges and 1973 K for the nose cap. Under these conditions (high temperature and low pressure), ceramics such as silicon carbide, used as a coating material to protect the carbon–carbon composites of the shuttle, is rapidly oxidized.

Many authors [1–9] have studied the oxidation of SiC at high temperatures (< 2100 K) but at atmospheric pressure (0.1 MPa), and as a consequence they always find a "passive" oxidation with the formation of a silica layer and a weight gain of the sample. At lower pressure, the oxidation is called "active" with vaporization of the oxides SiO and CO with a weight loss of the sample.

In the literature, many different values are reported for the transition between active and passive oxidation in the case of SiC [10–16]. Therefore, before conducting the experiments, a theoretical thermodynamic calculation was performed, based on the Wagner's model [17] used for SiC.

2. Theoretical thermodynamic approach

2.1. Molecular oxygen

The oxidation of SiC is performed in flowing air, thus the neutral carrier gas, nitrogen, is taken into account.

First, Eriksson's model (Solgasmix [18]) is used to determine the dominant gaseous species at the solid–gas interface. The equilibrium calculations are based upon the free-energy minimization method for constant temperature and pressure values. The constraints of the model are: closed system, mass conservation and Duhem's phase rule.

Before passivation by the silica layer, the solid–gas interface is composed of the solid silicon carbide layer and of the major gaseous species SiO, CO, O_2 and N_2 given by Solgasmix.

Second, Wagner's model is used. It is well suited because it takes into account the mass-transfer constraints (open system) and leads to the analytical determination of the transition point in terms of oxygen partial pressure in the bulk gas, for each temperature.

Let us consider the system SiC(s), SiO(g), CO(g), O_2(g) and N_2(g); the variance is equal to 4. For fixed temperature and pressure, the system is bivariant. In order that the system is entirely determined, it is necessary to impose two additional constraints given by the mass-transfer equations.

For each phase, the mass balance for each atomic compound is established and then the interface mass conservation (steady state). The flux density, J_i, of the compound i at the interface is expressed by Fick's law

$$J_i = -\frac{D_i}{\delta_i RT}(P_i^{\infty} - P_i^{w}) \quad (1)$$

where D_i is the mass transfer coefficient of i in the carrying gas N_2, $D_i = D_{i,N_2}$, δ_i the thickness of the boundary concentration layer, R the perfect gas constant, T the temperature, P_i the partial pressure of the species i in the bulk gas (P_i^{∞}) and at the interface (P_i^{w}).

0022–2461/92 $03.00 + .12

In the gaseous phase

$$(J_O^G) = 2J_{O_2}^G + J_{SiO}^G + J_{CO}^G \quad (2)$$

$$(J_{Si}^G) = J_{SiO}^G \quad (3)$$

$$(J_C^G) = J_{CO}^G \quad (4)$$

$$(J_N^G) = 2J_{N_2}^G \quad (5)$$

In the condensed phase

$$(J_O^S) = 0 \quad (6)$$

$$(J_{Si}^S) = J_{SiC}^S \quad (7)$$

$$(J_C^S) = J_{SiC}^S \quad (8)$$

$$(J_N^S) = 0 \quad (9)$$

Accounting for the principle of mass conservation at the interface, the following system is obtained:

$$\begin{cases} 2J_{O_2}^G + J_{SiO}^G + J_{CO}^G = 0 \\ J_{SiO}^G = J_{CO}^G \\ J_{N_2}^G = 0 \end{cases} \quad (10)$$

So, we have two independent relations which are the two constraints.

System 1 corresponds to

$$\begin{cases} J_{O_2}^G + J_{SiO}^G = 0 \\ J_{N_2}^G = 0 \end{cases} \quad (11)$$

$$\rightarrow \frac{D_{O_2}}{\delta_{O_2}}(P_{O_2}^\infty - P_{O_2}^w) + \frac{D_{SiO}}{\delta_{SiO}}(P_{SiO}^\infty - P_{SiO}^w) = 0 \quad (12)$$

With the two hypotheses: $P_{O_2}^w \approx 0$ (interface consumption) and $P_{SiO}^\infty = 0$ (boundary concentration layer), Equation 12 is reduced to

$$P_{O_2}^\infty = \frac{D_{SiO}}{\delta_{SiO}} \frac{\delta_{O_2}}{D_{O_2}} P_{SiO}^w \quad (13)$$

According to Wagner [17], the ratio of the thicknesses δ_{O_2} and δ_{SiO} can be expressed in a first approximation by

$$\delta_{O_2}/\delta_{SiO} = (D_{O_2}/D_{SiO})^{1/2} \quad (14)$$

This assumption is valid for a laminar flow, where the Reynolds number is less than 1.

Finally, Equation 13 is reduced to

$$P_{O_2}^\infty = \left(\frac{D_{SiO}}{D_{O_2}}\right)^{1/2} P_{SiO}^w \quad (15)$$

In the same way, as with $J_{O_2}^G = -J_{SiO}^G$, we have $J_{O_2}^G = -J_{CO}^G$. The oxygen partial pressure in the bulk is also given by

$$P_{O_2}^\infty = \left(\frac{D_{CO}}{D_{O_2}}\right)^{1/2} P_{CO}^w \quad (16)$$

Then the oxygen partial pressure is expressed in terms of thermodynamical parameters accounting for the equilibrium

$$SiC(s) + O_2(g) \rightleftharpoons SiO(g) + CO(g) \quad \Delta G_1^0 \quad (17)$$

Define the equilibrium constant, K_1, as

$$K_1 = \exp(-\Delta G_1^0/RT) = P_{SiO}^w(P_{CO}^w/P_{O_2}^w) \quad (18)$$

So, by introducing Equations 15 and 16 into Equation 18

$$P_{O_2}^\infty = \left(\frac{D_{SiO}}{D_{O_2}}\right)^{1/4} \left(\frac{D_{CO}}{D_{O_2}}\right)^{1/4} K_1^{1/2}(P_{O_2}^w)^{1/2} \quad (19)$$

In the present case $P_{O_2}^\infty$ is an unknown parameter and we wish to express this oxygen partial pressure only in terms of thermodynamic and diffusion parameters.

Just at the transition, Equilibrium 20 is also valid

$$SiC(s) + 3/2\,O_2(g) \rightleftharpoons SiO_2(s) + CO(g) \quad \Delta G_2^0 \quad (20)$$

with

$$K_2 = \exp(-\Delta G_2^0/RT) = P_{CO}^w(P_{O_2}^w)^{-3/2} \quad (21)$$

From Equation 21 we have the interfacial oxygen partial pressure to introduce into Equation 19 and by using the Equation 16 we finally obtain the oxygen partial pressure of transition in the bulk

$$P_{O_2}^\infty = \left(\frac{D_{SiO}}{D_{O_2}}\right)^{3/8} \left(\frac{D_{CO}}{D_{O_2}}\right)^{1/8} K_1^{3/4} K_2^{-1/2} \quad (22)$$

In the case of an ideal gas at low density, the diffusion coefficient can be approximated by the Chapman–Enskog theory [19]. The relation is

$$D_{i,j} = 0.001\,8583 \left[\left(\frac{1}{M_i} + \frac{1}{M_j}\right) T^3\right]^{1/2} \Big/ P\sigma_{ij}^2 \Omega_{ij} \quad (23)$$

where P is the total pressure, σ_{ij} the Lennard–Jones parameter, Ω_{ij} the dimensionless function representative of the collision integral. In addition, the collision diameter may be expressed by the empirical relations $\sigma_{ij} = 1/2(\sigma_i + \sigma_j)$ and the intermolecular energy of attraction by $\varepsilon_{ij} = (\varepsilon_i \varepsilon_j)^{1/2}$; the latter parameter is needed for the Ω_{ij} calculation [20].

Table I gives the values of σ_{ij}, Ω_{ij} and D_{ij} for SiO, CO, O_2, O and N_2. Consequently, the ratio D_{SiO}/D_{O_2} and D_{CO}/D_{O_2} are, respectively, 0.44 and 0.99 in the case of N_2 as the inert gas.

With these data, Equation 22 becomes

$$P_{O_2}^\infty = 0.734\, K_1^{3/4} K_2^{-1/2} \quad (24)$$

The values given in Table I for other inert gases such as argon and helium are reported for the calculation of the ratios D_{SiO}/D_{O_2} or D_{CO}/D_{O_2} for the data of Hinze

TABLE I Values of the Lennard–Jones parameters, the integral collision and the diffusion coefficient, at 2000 K

i	j	σ_i (nm)	σ_{ij} (nm)	Ω_{ij}[a]	D_{ij} ($cm^2 s^{-1}$)
SiO	N_2	0.478[b]	0.423	(1.00)	2.24
CO	N_2	0.359	0.364	0.6645	5.04
O_2	N_2	0.343	0.356	0.6666	5.09
O	N_2	0.256	0.312	(1.00)	5.35
SiO	Ar	–	0.410	(1.00)	1.66
CO	Ar	–	0.350	(1.00)	2.18
O_2	Ar	–	0.343	(1.00)	2.13
SiO	He	–	0.387	(1.00)	5.80
O_2	He	–	0.320	(1.00)	8.62

[a] Ω_{ij} = (1.00) when unknown (rigid-sphere model).

[b] Calculated from $\sigma_i = (2r_i + 1.1)10$ nm (semi-empirical, from [19]) with the following values $\sigma_{N_2} = 0.368$ nm, $\sigma_{Ar} = 0.342$ nm and $\sigma_{He} = 0.258$ nm.

TABLE II Temperatures and pressures for the active to passive transition (theoretical calculation and literature data)

T (K)	$P^{\infty}_{O_2}$ (Pa)				
	Present work	[11] eqC-eqA	[13]	[16]	[15]
1373	0.2	0.08–2.4	0.5	0.005[a]	0.14[a]
1473	9	0.72–16	4	0.09[a]	0.9[a]
1573	57	5.2–101	23	1[a]	4[a]
1673	297	32–583	103	10	17
1773	1247	202–2430	544	75	60
1873	4410	723–8357[a]	1420	440	182
1973	13628	2607–26406[a]	5270	2163[a]	493[a]
2073	37558	8277–74393[a]	15400[a]	9116[a]	1215[a]

[a]Extrapolated from the given values.

and Graham (argon [16]) and Wagner (helium [17]). The calculation of D_{ij} requires the values of σ_{ij}, and Ω_{ij} (or for SiO, $\Omega_{SiO,j}$) is unknown, so we choose a value of 1 equivalent to the rigid-sphere model in the kinetic theory of gases [19].

The exact values of $\Omega_{CO,Ar}$, $\Omega_{O_2,Ar}$ and $\Omega_{O_2,He}$ are known but we used 1.00, because this is the value used by Hinze and Wagner for the calculation of their diffusion coefficients.

Table II gives the values of the temperatures and oxygen partial pressures in the bulk gas for the active to passive transition zone. The calculations are based upon the data of the JANAF tables [21] and the diffusion coefficients given in Table I. The theoretical results of Gulbransen and Jansson [11] and Singhal [13], and the experimental values of Vaughn and Maahs [15] and Hinze and Graham [16] are also reported.

A large scatter is seen between the different theoretical and experimental values of the oxygen partial pressure. First, the experimental results of Hinze and Graham and Vaughn and Maahs are very low by comparison with all the theoretical values. Second, the disparity between our theoretical values and those of Gulbransen and Jansson [11] and Singhal [13] is due to the method of calculation of the diffusion coefficients and also to the thermodynamical data (JANAF tables 1971 and 1985). For example, for Singhal, the ratio D_{SiO}/D_{O_2} is equal to 0.16 and for the present case this ratio is 0.44, which leads to a factor difference of nearly 2 on the pressure. Gulbransen and Jansson describe the transition with three possible equilibria; the values given in Table II are the extreme ones (C and A). The three equilibria A, B and C [11] depend on the oxidation gaseous products SiO(g) + CO(g) (A) or SiO(g) (B) or CO(g) (C). The dominant gaseous species at these temperature and pressure conditions are SiO and CO so it is only Equilibrium A which describes the transition.

Here the importance of the value of the integral collision Ω_{ij} on the diffusion coefficient ratio may be pointed out. It could be increased by a factor of 2 depending on whether Ω_{ij} is equal to 1.00 or is lower.

2.2. Atomic oxygen

The same calculation can be made for atomic oxygen. System 1 is changed by

$$\begin{aligned} J^G_O + J^G_{CO} + J^G_{SiO} &= 0 \\ J^G_{CO} &= J^G_{SiO} \\ J^G_{N_2} &= 0 \end{aligned} \tag{25}$$

With the same hypothesis, we obtain for Equations 15 and 16

$$P^{\infty}_O = 2\left(\frac{D_{SiO}}{D_O}\right)^{1/2} P^w_{SiO} \tag{26}$$

$$P^{\infty}_O = 2\left(\frac{D_{CO}}{D_O}\right)^{1/2} P^w_{CO} \tag{27}$$

The two equilibria are

$$SiC(s) + 2O(g) \rightleftharpoons SiO(g) + CO(g) \quad \Delta G^0_3 \tag{28}$$

$$SiC(s) + 3O(g) \rightleftharpoons SiO_2(s) + CO(g) \quad \Delta G^0_4 \tag{29}$$

with

$$K_3 = \exp(-\Delta G^0_3/RT) = P^w_{SiO}[P^w_{CO}/(P^w_O)^{-2}] \tag{30}$$

$$K_4 = \exp(-\Delta G^0_4/RT) = P^w_{CO}(P^w_O)^{-3} \tag{31}$$

The same argument is used and then we finally obtain the relation giving the oxygen partial pressure in the bulk gas

$$P^{\infty}_O = 2\left(\frac{D_{CO}}{D_{SiO}}\right)^{1/8}\left(\frac{D_{SiO}}{D_O}\right)^{1/2} K_3^{3/4} K_4^{-1/2} \tag{32}$$

or

$$P^{\infty}_O = 1.44\, K_3^{3/4} K_4^{-1/2} \tag{33}$$

In terms of $P^{\infty}_{O_2}$ equivalent ($P^{\infty}_{O_2} = 0.5P^{\infty}_O$), the same result for the transition is obtained as in the case of molecular oxygen. This was described in yet another manner (variant of the thermodynamical approach based on their observed oxidation probabilities) by Rosner and Allendorf [14].

Fig. 1 gives the theoretical curve $\mathrm{Log}\, P^{\infty}_i = f(1/T)$ obtained for O_2 and O, and the curves of Gulbransen and Jansson [11], Singhal [13], Vaughn and Maahs [15] and Hinze and Graham [16].

3. Experimental procedure

The experimental apparatus is shown in Fig. 2. It is composed of a cylindrical vessel (1) of 500 mm high and 50 mm diameter which crosses the wave guide (3). Inside the vessel, a zirconia tube with a sample holder supports the materials. The microwave generator works at a constant power of 300 W at a frequency of 2450 MHz. A coaxial cable links the generator and the wave guide. The plasma is pink with a yellow–green post-discharge characteristic of an air plasma. The presence of atomic oxygen was detected by emission spectroscopy. This device is placed at the focus of a solar furnace. The heat fluxes can reach 4.5 MW m^{-2}, thus elevated temperatures on materials such as SiC may be obtained. A pressure regulator (7) and a pressure gauge (8) are used in order to control precisely the pressure during the experiment. An optical pyrometer (9) equipped with a filter centred at 5.5 μm

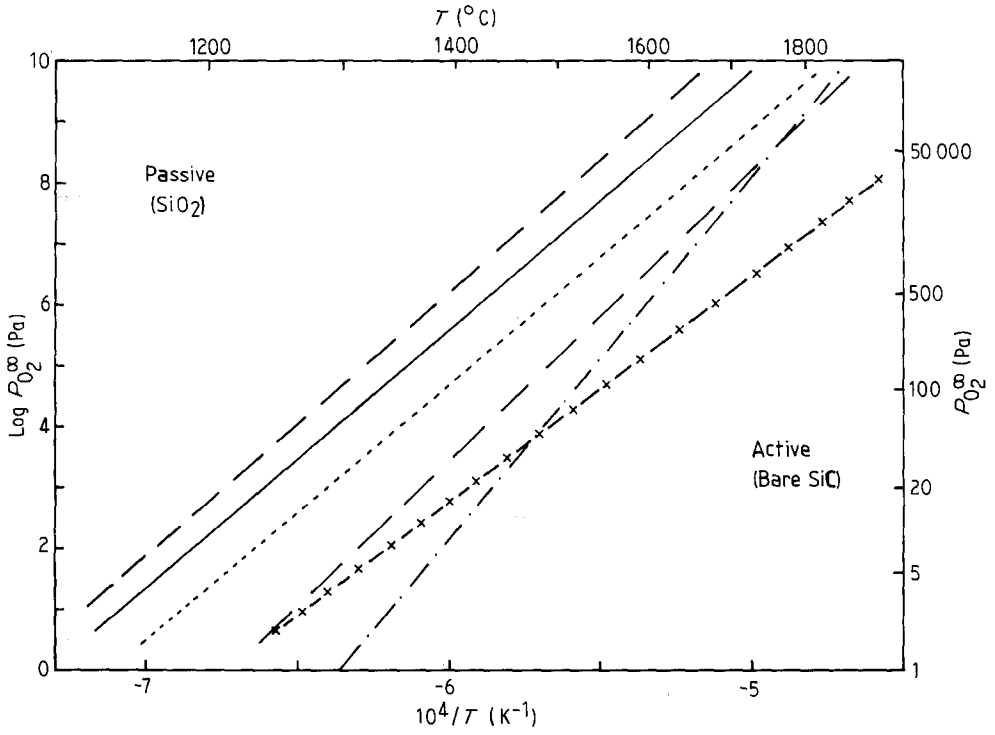

Figure 1 Theoretical curves of oxygen partial pressure versus temperature from (———) present work, (— — —) [11], (- - -) [13], (—·—) [16], (—×—) [15].

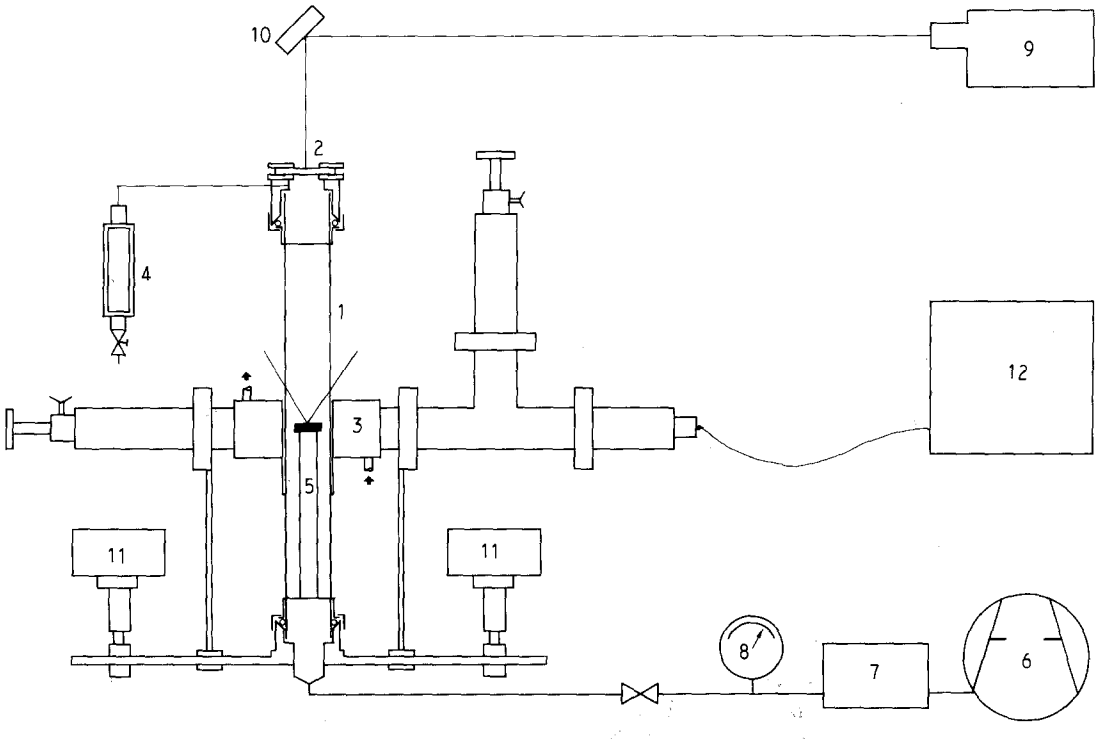

Figure 2 The experimental apparatus: 1, silica vessel; 2, CaF_2 window; 3, wave guide; 4, flowmeter; 5, sample-holder tube; 6, vacuum pump; 7, pressure regulator; 8, pressure gauge; 9, optical pyrometer; 10, mirror; 11, support; 12, microwave generator.

gives an output voltage linearly proportional to the colour temperature. The measure is performed with a mirror (10) and a CaF_2 window (2). The correction of the temperature due to the emittance is done a posteriori with a value of $\varepsilon(\lambda = 5.5\ \mu m) = 0.90$ for SiC and SiO_2 [22]. The uncertainty in the temperature due to the correction of emittance is 3% at 1773 K for a variation of 5% on ε.

4. Results

After the theoretical determination of the temperature and pressure conditions for the transition between active and passive oxidation, the experiments given in Table III were carried out.

The samples were sintered α-SiC (6H) containing, as major impurities, 1% B and < 2000 p.p.m. Si and SiO_2.

TABLE III Experimental points

Sample	Under molecular oxygen O_2(g)					Under atomic oxygen O (g)						
	A	B	C	D	E	A′	B′	C′	D′	F′	G′	H′
T (K)	1653	1663	1673	1767	1779	1666	1683	1676	1781	1806	1869	1948
$P^{\infty}_{O_2}$ (Pa)	200	400	700	1000	2100	200	400	700	1000	1000	1000	1000

The sample's dimensions were 25 mm diameter and 3 mm high. On the upper face (exposed to the solar flux) where the temperature was measured, the sample was polished using a 6 μm diamond polishing compound, then cleaned ultrasonically in methanol and dried before testing.

4.1. Experimental protocol

The pressure and gas-flow conditions (constant, equal to 1.06 $cm^3 s^{-1}$) were realized and the pressure stabilized before each experiment.

For the experiments performed under plasma, the plasma was started after the pressure stabilization and before isolation of the sample. By the gradual opening of the shutter placed between the sample and the concentrated solar flux, a temperature increase of 4 $K s^{-1}$ was selected, then the temperature level was maintained for 360 or 420 s, according to the experiment, and sample cooling was regulated at 2 $K s^{-1}$.

The modification of the sample was controlled by weighing before and after the test run. The presence of a silica layer was determined by weighing (mass gain), X-ray diffraction (XRD) and Auger spectroscopy.

The experimental points are given on Fig. 3 with the theoretical curve corresponding to the active to passive transition.

4.2. Experiments under molecular oxygen

The experiments symbolized by the letters A, B, C, D and E, were performed under molecular oxygen (flowing air). For Samples A, B and D, after the oxidation test run, the surface was bare and was composed only of SiC. This proves that for these three tests, the oxidation is active with vapourization of the two oxides SiO and CO according to Equilibrium 17 with respective weight losses of 2%, 2.2% and 3.6%.

In Samples C and E, the surface was covered with a thin passive silica layer. The weight gain was very weak but the presence of silica was revealed by XRD; it was α-cristobalite with a peak at $2\theta = 21.95°$ ((1 0 1)).

Except for Sample B, which might be covered with a silica layer (possibly due to the precision on the temperature measurement), the experiments done under molecular oxygen were in good agreement with the thermodynamical calculation. A precision of 3% was obtained.

4.3. Experiments under dissociated oxygen

For Samples A′, B′, C′, D′ and E′, the oxidation was passive with a formation of a very thin silica layer. A rough estimation of the thickness of Sample A′ by Auger spectroscopy gives about 100–150 nm. Fig. 4

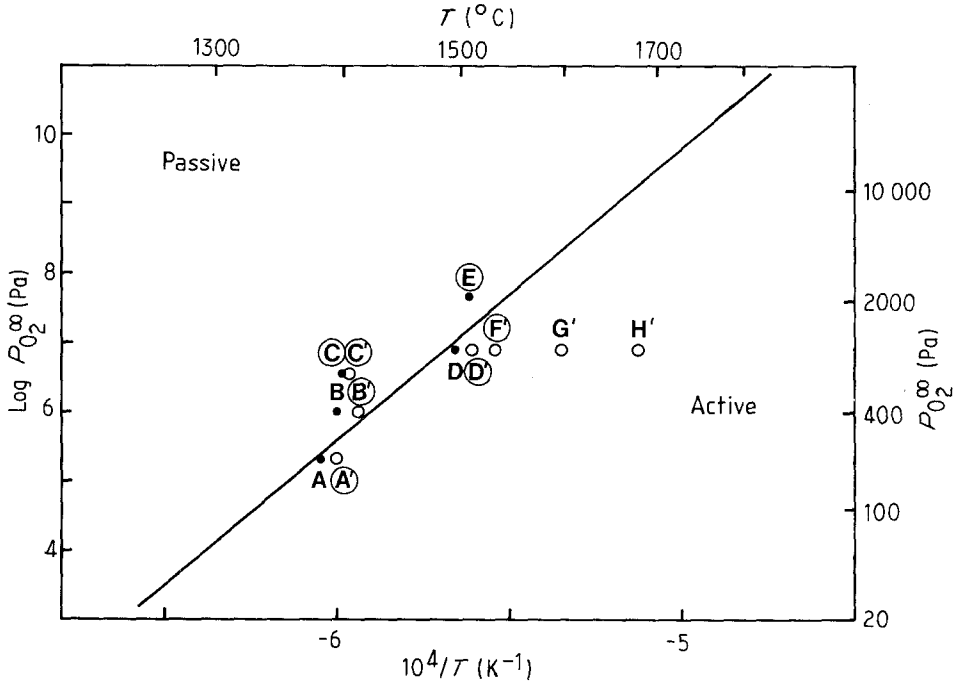

Figure 3 Oxygen partial pressure versus temperature. Theoretical straight line for the transition (thermodynamical calculation) and experimental points (A (●) under molecular oxygen and A′ (○) under atomic oxygen). The letters surrounded by a circle represent the samples with a passive silica layer after oxidation.

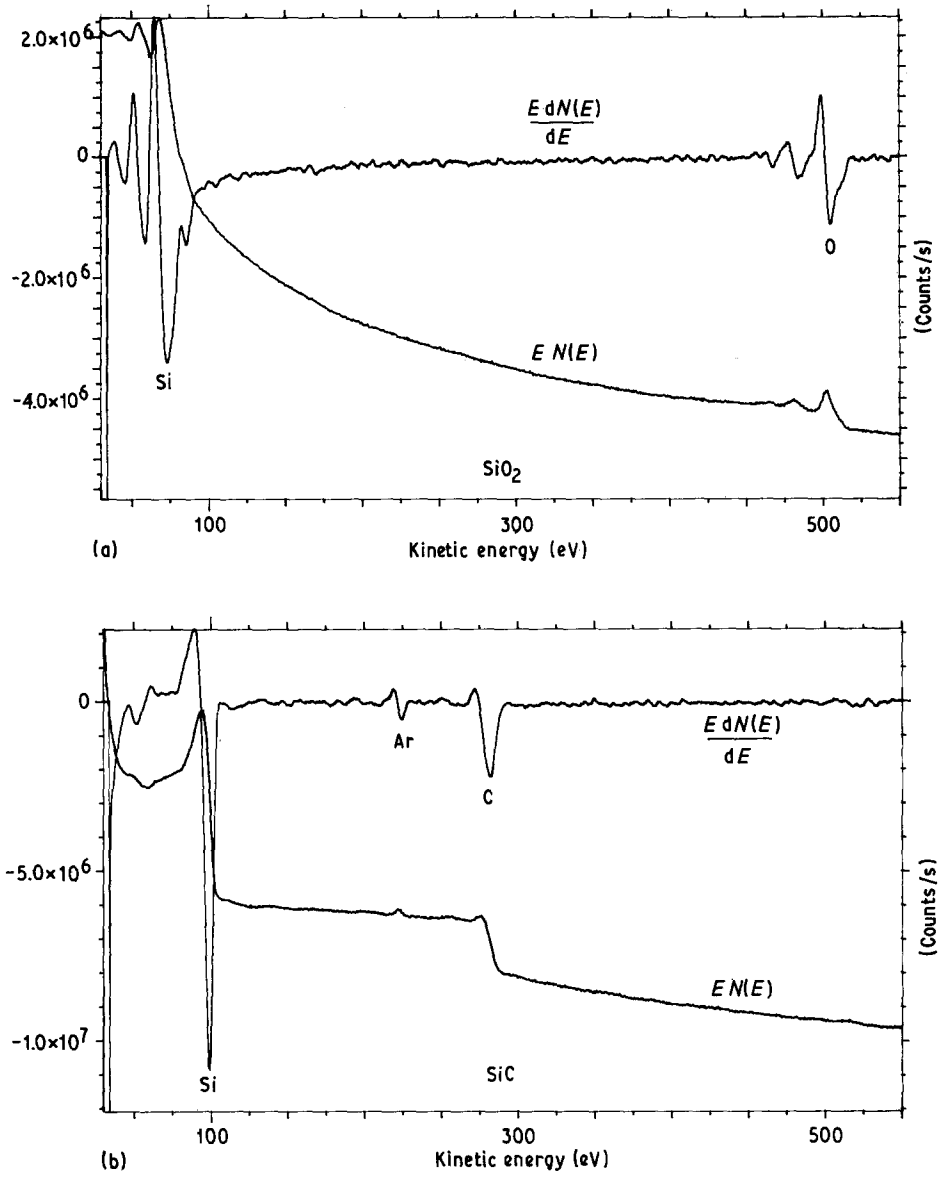

Figure 4 Auger spectroscopy data for Sample A′ (under atomic oxygen) after (a) 15 min, and (b) 70 min Ar^+ etching.

represents two Auger spectra taken on A′. Spectrum (a) is obtained after 15 min Ar^+ etching and reveals the SiO_2 layer, and Spectrum (b) represents the SiC materials after perforation of the silica layer (after 70 min Ar^+ etching).

For Samples G′ and H′, with surface temperatures of 1869 and 1948 K, respectively, there was vaporization of SiO and CO with weight losses of 2.5% and 4%.

With atomic oxygen, the active to passive transition was observed at a higher temperature for the same pressure, or at a lower pressure for the same temperature than for an O_2 atmosphere, i.e. the dissociation significantly enlarges the P–T domain characterized by the presence of a protective condensed film of silica.

This was observed by Rosner and Allendorf [14] in the case of very low pressures (10^{-2}–10 Pa) and at high temperatures (1750–2400 K) on pyrolytic SiC. According to these authors, in contradiction to the thermodynamical prediction, for any temperature below 2100 K, passive behaviour occurs for a much lower reactant pressure with O(g) than with O_2(g). A difference exceeding two orders of magnitude at the lowest temperature investigated (1750 K) was observed.

According to our results, the discrepancy reaches about a factor four at the same temperature level.

The difference observed between the dissociated and undissociated oxygen behaviour strongly tends towards a kinetic reaction control.

Fig. 5 shows two photographs of silica layers obtained by optical microscopy. For nearly the same position opposite to the transition straight line (40 K), (a) and (b) represent, respectively, Samples E oxidized under O_2(g) and F' oxidized under O(g).

For Sample E, the silica layer is thick and it shows two phases: crystallized (α-cristobalite) and amorphous revealed by X-ray diffraction.

For Sample F', the silica layer is smaller with some bubbles. Only Auger spectroscopy can show up the silica, the X-ray diffraction being not so sensitive for the thickness of the oxide layer.

5. Conclusion

The active to passive transition in the oxidation of silicon carbide in flowing air, under molecular and

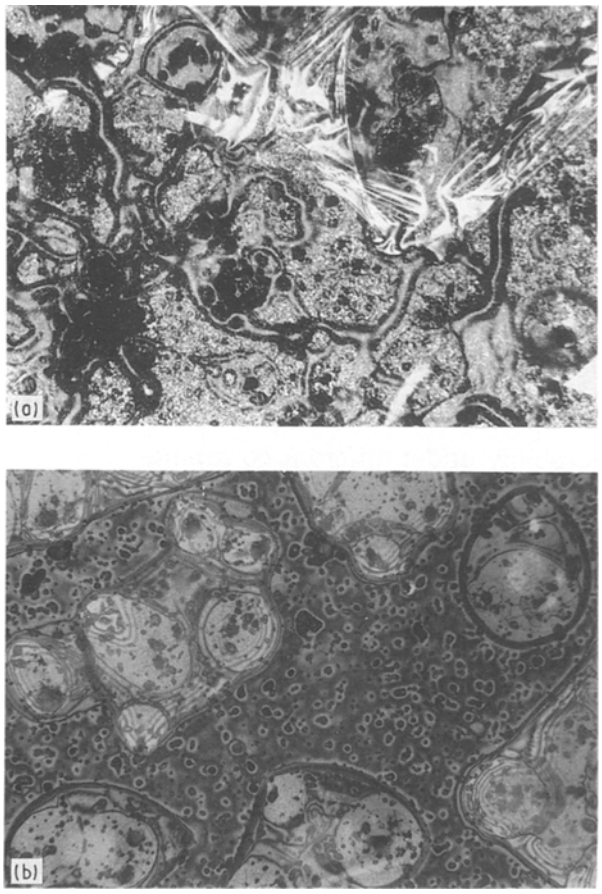

Figure 5 Optical micrographs of silica layers on Samples (a) E, × 200 and (b) F′, × 500.

dissociated oxygen is first determined by a thermodynamic calculation based on Wagner's model [17] extended to SiC. The thermodynamic equilibrium being the model hypothesis, the study shows clearly that no difference exists between $O_2(g)$ and O(g) in the case of the oxidation of SiC.

An experimental apparatus designed for testing samples at high temperatures (solar furnace with concentrated flux) and low pressure under molecular and plasma atmospheres (generated by microwaves) is used to test sintered α-SiC samples, in the case of low flow gas conditions (1 $cm^3 s^{-1}$).

Under undissociated oxygen, the experimental results are consistent with the thermodynamic prediction. On the contrary, under dissociated oxygen, an enlargement of the region of formation of a passive silica layer is observed. The transition occurs at lower pressures for the same temperature range than in the case of the molecular atmosphere.

According to these results, a kinetics control of the reaction may be assumed in the case of atomic oxygen and also under molecular oxygen, in spite of the agreement between theoretical and experimental results in the case of molecular oxygen.

The behaviour observed under dissociated oxygen is very useful, particularly for the thermal protective coatings of the space shuttle which, during atmospheric reentry, encounters such temperature and pressure levels, because the coating can maintain its protective function by the passive oxide layer formation.

In the future, a better characterization of the plasma must be done. We also wish to study the effect of an increase in the gas flow and to determine the experimental transition zone in the case of atomic oxygen.

References

1. K. MOTZFELDT, *Acta Chem. Scand.* **18** (1964) 1596.
2. S. C. SINGHAL, *J. Mater. Sci.* **11** (1976) 1246.
3. J. A. COSTELLO and R. E. TRESSLER, *J. Amer. Ceram. Soc.* **64** (1981) 327.
4. J. W. PALMOUR, H. J. KIM and R. F. DAVIS, *Mater. Res. Soc. Symp. Proc.* **54** (1986) 553.
5. W. VOLKER, *cfi/Ber. DKG* **63** (1986) 385.
6. G. H. SCHIROKY, *Adv. Ceram. Mater.* **2** (1987) 137.
7. V. A. LAVRENKO, E. A. PUGACH, S. I. FILIPCHENKO and Y. G. GOGOTSI, *Oxid. Metals* **27** (1987) 83.
8. T. NARUSHIMA, T. GOTO and T. HIRAI, *J. Amer. Ceram. Soc.* **72** (1989) 1386.
9. K. E. SPEAR, R. E. TRESSLER, Z. ZHENG and H. DU, in "Proceedings of the Symposium on Corrosion and Corrosive Degradation of Ceramics", Ceramic Science and Technology Congress, Anaheim (CA), 31 October–3 November 1989.
10. E. A. GULBRANSEN, K. F. ANDREW and F. A. BRASSART, *J. Electrochem. Soc.* **113** (1966) 1311.
11. E. A. GULBRANSEN and S. A. JANSSON, *Oxid. Metals* **4** (1972) 181.
12. J. E. ANTILL and J. B. WARBURTON, *Corrosion Sci.* **11** (1971) 337.
13. S. C. SINGHAL, *Ceram. Int.* **2** (1976) 123.
14. D. E. ROSNER and H. D. ALLENDORF, *J. Phys. Chem.* **74** (1970) 1829.
15. W. L. VAUGHN and H. G. MAAHS, *J. Amer. Ceram. Soc.* **73** (1990) 1540.
16. J. W. HINZE and H. C. GRAHAM, *J. Electrochem. Soc.* **123** (1976) 1066.
17. C. WAGNER, *J. Appl. Phys.* **29** (1958) 1295.
18. G. ERIKSSON, *Chem. Scripta* **8** (1973) 100.
19. R. B. BIRD, W. E. STEWART and E. N. LIGHTFOOD, "Transport phenomena" (Wiley, New York, 1960) pp. 508–13.
20. J. W. HASTIE, "High temperature vapors – Science and Technology" (Academic Press, New York, 1975) pp. 115–22.
21. M. W. CHASE, J. R. DAVIES *et al.*, "JANAF thermodynamical tables", 3rd Edn, *J. Phys. Chem. Ref. Data* **14**, suppl. 1 (1985).
22. Y. S. TOULOUKIAN and D. P. De WITT, "Thermal radiative properties – Non metallic solids", Vol. 8 (Plenum, New York, 1972).

Received 4 October 1990
and accepted 20 March 1991